PROGRESS IN PHOTOVOLTAICS: RESEARCH AND APPLICATIONS
Prog. Photovolt: Res. Appl. **2012; 20**:135–142
Published online 27 May 2011 in Wiley Online Library (wileyonlinelibrary.com). DOI: 10.1002/pip.1123

ACCELERATED PUBLICATION

Antireflection and light trapping of subwavelength surface structures formed by colloidal lithography on thin film solar cells

Ping-Chen Tseng[1], Min-An Tsai[2], Peichen Yu[1]* and Hao-Chung Kuo[1]

[1] Department of Photonics and Institute of Electro-Optical Engineering, National Chiao Tung University, Hsinchu 30010, Taiwan, R.O.C
[2] Department of Electro-physics, National Chiao Tung University, Hsinchu 30010, Taiwan, R.O.C

ABSTRACT

In this paper, we present a novel design of a surface nanostructure that suppresses the reflectivity and provides forward diffraction for light trapping. The structure under study comprises periodic nanoislands fabricated using self-assembly polystyrene spheres, which are applicable to large-area fabrication. We also show preliminary fabrication results of the proposed structure. The periodic nanoislands reduce the reflectivity through gradient effective refractive indices and enhance light trapping through diffraction in a periodic structure. We first systematically study the antireflection and light trapping effects using a rigorous coupled-wave analysis and then calculate the short-circuit current density of a 2-μm-thick crystalline silicon with periodic nanoislands and an aluminum back reflector. The optimum short-circuit current density with periodic nanoislands achieves 25 mA/cm^2 theoretically, which shows a 76.9% enhancement compared with that of bare silicon. Moreover, the structure also provides superior photocurrent densities at large angles of incidence, compared with conventional antireflection coatings. Copyright © 2011 John Wiley & Sons, Ltd.

KEYWORDS

thin-film solar cell; light trapping; antireflection; colloidal lithography

***Correspondence**

Peichen Yu, Electro-Optics, NCTU, 1001 University Road, Hsinchu, Taiwan 300.
E-mail: yup@faculty.nctu.edu.tw

Received 12 January 2010; Revised 28 September 2010

1. INTRODUCTION

Recently, solar cell development has been a major study around the world, especially for thin-film solar cells. Because of little material usage and low cost, thin- film solar cells have become the main stream in green energy. However, the efficiency is currently not comparable with that of thick crystalline solar cells owing to limited sunlight harvested by the thin absorbing layer. In particular, thin-film crystalline silicon (c-Si) solar cells fabricated with a thickness of less than 10 μm makes it difficult to absorb the long-wavelength portion of solar power because of weak optical absorption. Therefore, improving the spectral absorption to long wavelengths is a critical issue for efficiency enhancement. In general, there are two approaches to enhance solar power harvest for thin films: light entry enhancement and light trapping for the long-wavelength region.

Light entry enhancement is the first step toward a high conversion efficiency of a solar cell. An antireflection (AR) coating is usually implemented to enhance the optical transmission for specified wavelengths. However, a good coating requires several dielectric layers with specific refractive indices and thicknesses to achieve broadband antireflection, which increases the cost. Surface texturing is another way to facilitate the photon entry for silicon (Si) cells. However, the texturing is usually achieved by chemical etching, which results in micro-scale structures. Therefore, the method is not applicable for thin-film solar cells. In addition, random nanostructures have also been added to the c-Si surface to serve as omnidirectional antireflection layers [1].

Light trapping is the other alternative to improve the optical absorption of thin-film cells. With such a thin thickness of absorbers, the long wavelength photons suffer from insufficient optical path lengths, leading to low quantum efficiency in the near-infrared. Typically, enhancing light trapping in thin-film solar cells is achieved by using a textured back-reflector that scatters light within the absorber layer to increase the optical path length for photons.

However, the roughened structure usually has a dimension of several micrometers, which is too large to be used in thin films. Several reports on light-trapping research have been concentrated on engineering photonic crystal structures as the back-reflector for solar cells. P. Bermal *et al.* have theoretically demonstrated the absorption enhancement of Si with one-dimensional, two-dimensional and three-dimensional woodpile photonic crystals as the back-reflector [2]. Because Si with a thickness of a few micrometers can be obtained from a silicon-on-insulator system, L. Zeng *et al.* have experimentally shown the enhanced efficiency of a 5-μm-thick c-Si with a designed back-reflector composed of grating and distributed Bragg reflector (DBR) structures [3]. The design of the grating and DBR back-reflector has also been theoretically analyzed and optimized for silicon with a-few-micrometer thickness [4]. D. Zhou and R. Biswas have theoretically investigated that the enhancement arose from hydrogenated amorphous silicon with a two-dimensional nanorod photonic crystal incorporating a DBR structure [5]. The idea of photonic-crystal back reflectors can only passively trap the "leftover" photons without increasing the photon entry, which limits the efficiency enhancement. Herein, we propose a novel surface structure that provides both antireflection and light trapping to enhance the absorption of a 2-μm-thick c-Si cell, which can be obtained from either silicon-on-insulator or crystalline-silicon-on-glass systems [6]. We further show that the structure can be easily fabricated for large areas using colloidal lithography [7,8].

2. SIMULATION STRUCTURE

The proposed structure was implemented using polystyrene (PS) nanospheres as sacrificial masks. The schematic and preliminary fabrication results are shown in Figure 1. In the fabrication process, PS spheres with a diameter of 600 nm were first spin-cast on a Si substrate by adjusting the speed of a spin coater (800–3600 rpm) and the surfactant concentration to form a close-packed structure, as shown in the top scanning electron microscopic image in Figure 1. Oxygen plasma treatment was subsequently employed to slightly shrink the PS spheres using a reactive ion etcher under a radio-frequency power of 250 W at 5 mtorr pressure for 60 s. Next, the two-dimensional hexagonal colloidal array served as a self-assemble template for titanium dioxide (TiO_2) deposition. The deposition of TiO_2 with a height of 120 nm was performed at ~100°C to avoid melting the PS spheres using an electron-beam evaporation system. Thereafter, the PS spheres were removed by dipping the substrate into acetone with sonification for 5 min, which naturally left the hexagonal-arranged periodic nanoislands on the surface, as shown in the bottom scanning electron microscopic image in Figure 1. The height of TiO_2 nanoislands was therefore limited by the radius of polystyrene spheres to facilitate the lift-off process. The parabolic-triangular-pyramidal (PTP) nanoislands were periodically arranged on the surface of the solar cell, which were systematically investigated for the reflection reduction and diffraction effects. Finally, the absorption efficiencies of 2-μm-thick c-Si cells with various sphere diameters, D and heights of the TiO_2 islands, H were optimized. The calculated parameters included the sphere diameter D, and the aspect ratio of TiO_2 islands, X ($X = H/D$, and $H \leqq D/2$). The numerical simulation was conducted using a rigorous coupled-wave analysis (RCWA), which exploits a Fourier expansion of the periodic structure to solve Maxwell's equations [9]. A commercial implementation, RSoft DiffractMOD™ (RSoft Design Group, Inc., Ossining, New York, USA), was used to perform the calculation of

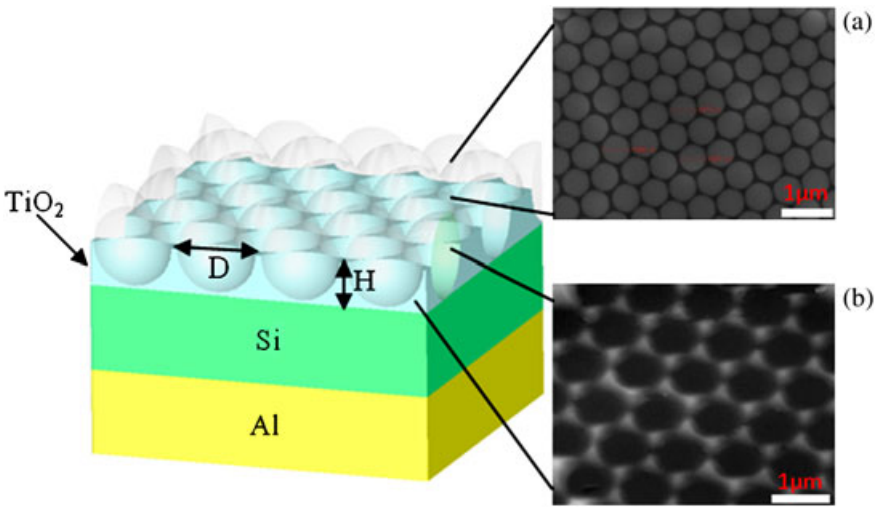

Figure 1. The periodic nanoisland structure on thin-film silicon with an aluminum back-reflector. The scanning electron micrographs show the periodically arranged polystyrene spheres in a hexagonal lattice (a) and the remaining nanoislands after titanium dioxide (TiO_2) deposition and nanosphere lift-off (b).

DOI: 10.1002/pip

the proposed structure. Several researches have successfully matched the experimental results with RCWA simulations [10,11]. The optical constants of the materials used in the simulation were obtained from Hale and Querry [12]. The incident plane-wave was assumed to be 45-degree polarized to simulate randomly polarized sunlight.

3. SURFACE REFLECTION

The surface reflectivity, which determines the amount of light that enters a cell, is the most important factor for the power conversion efficiency. The proposed island structure functions as broadband antireflection layers based on the effective medium theory, which describes the effective refractive index (RI) of the structure that is composed of different materials. The effective RI varies vertically with respect to the air fraction in the deposited material in each horizontal layer. For TiO_2 nanoislands, the air fraction (the cross-sectional area of lifted polystyrene spheres) in each layer within a period is expressed as $f_{\text{air}}(z) = 2\pi r^2(z)/\sqrt{3D^2}$, where $r = \sqrt{(D/2)^2 - (D/2 - z)^2}$. The material fraction is therefore, $f_{\text{mat}}(z) = 1 - f_{\text{air}}(z)$. The effective RI can then be estimated by using Bruggman's theory [13]. Here, the deposited material is taken as TiO_2, which has a higher refractive index ($n \sim 2.8$) than other transparent conducting oxides. The choice of material with a high refractive index is to approach that of Si, as the RIs are gradually changed by means of the structural profile. The effective RI in each layer is gradually decreased away from that of the Si surface, and finally is equivalent to that of air. The PTP nanoislands therefore reduce the surface reflection, according to Fresnel's equation, $R = (n_1 - n_2/n_1 + n_2)^2$, where the reflectivity R results from an interface between two materials with RIs of n_1 and n_2 [14].

To study the surface reflectivity, an infinitely thick Si layer was assumed to avoid multiple reflections and interferences between top and bottom surfaces. The schematic structure is shown in Figure 2. Figure 3 shows the calculated spectral reflectivity of nanoislands with a constant height $H = 300$ nm and various sphere diameters and bare Si with a 78-nm-thick single-layer silicon-nitride AR coating. For silicon-based solar cells (where $n \approx 3.5$), silicon nitride ($n \approx 1.91$) is commonly employed, although the refractive index roughly corresponds to the geometric mean of that of silicon and air [15]. The calculated reflectivity includes high-order modes from −4 to +4, where the diffracted power remains significant. Compared with the reflectivity of bare Si and Si with a single-layer AR coating, the nanoisland structure suppresses the surface reflection over the entire absorption spectrum of Si. Interestingly, the structure inhibits the surface reflection greatly at certain wavelengths where the reflectivity approaches zero. At these valleys, the structure functions as antireflection layers, which specifically shift the phase of the incident wave by 180°. The reduced reflectivity in the short-wavelength region, where the absorption of Si layer is high, contributes more photons for the electron hole pair generation than Si with a single-layer AR coating. Similarly, the suppressed reflectivity at the long-wavelength region enhances the photon entry for subsequent light trapping, which will be discussed in the next section.

To harness the most sun power into the Si layer, we calculate the average reflectivity with respect to the aspect ratio X and the sphere diameter D, weighted by the AM1.5 G solar spectrum (ASTM International, West Conshohocken, Pennsylvania, USA). The equation is written as follows:

$$\langle R \rangle = \frac{\int_{350\text{nm}}^{\lambda g} R_{\text{island}}(\lambda) I_{\text{AM1.5 G}}(\lambda) \mathrm{d}\lambda}{\int_{350\text{nm}}^{\lambda g} R_{\text{ref}}(\lambda) I_{\text{AM1.5 G}}(\lambda) \mathrm{d}\lambda}, \quad (1)$$

where R_{island} indicates the reflectivity of silicon with surface PTP nanoislands, R_{ref} is the reflectivity of silicon with a 78-nm-thick single-layer AR coating, which has a minimum average reflectivity, and $I_{\text{AM1.5G}}$ is the solar photon flux density under the condition of air mass 1.5 global [16]. The spectrum of interest ranges from 350 nm to λ_g, where $\lambda_g = 1100$ nm corresponds to the wavelength of Si bandgap. The result shown in Figure 4 indicates that when $X > 0.3$, the PTP islands exhibit a better antireflection property than the optimized single-layer AR coating. The minimum reflection is obtained at $D = 420$ nm, $X = 0.5$, where the reflection is suppressed by 60.5%. In general, a high aspect ratio X results in low surface reflection owing to a slow gradient of the effective RIs. Therefore, the structure can sufficiently reduce the surface reflectivity.

4. FORWARD DIFFRACTION

For low-energy photons, optical absorption is not sufficient because of intrinsically low absorption coefficients of the Si layer despite the increased transmitted photons. In the proposed structure, the nanoislands serve not only as the antireflection layers but also as a two-dimensional hexagonal grating on the surface. The close-packed spheres have formed hexagonal air holes after the lift-off of PS spheres and left the periodically arranged islands. Once the light enters a solar cell with a surface grating, it propagates through the solar cell at a particular diffraction angle based on the conservation of photon momentum. As nanoislands are divided into a number of thin layers vertically, each with a refractive index $n(x)$, the structure can be perceived as hexagonal gratings stacked up along the z-axis. The theoretical analysis of a hexagonal photonic crystal design was discussed in Ochiai and Sakoda [17]. The relevant issue for sufficient light trapping is the diffraction efficiencies for the high-order modes, that is, orders other than $(m, n) = (0, 0)$, where m and n denote the diffraction orders in x and y directions, respectively. The light distributed among the high orders, particularly, $(m, n) \neq (0, 0)$, propagates through Si at oblique angles, ϕ_{mn}. For an infinitely thick Si layer, the optical path

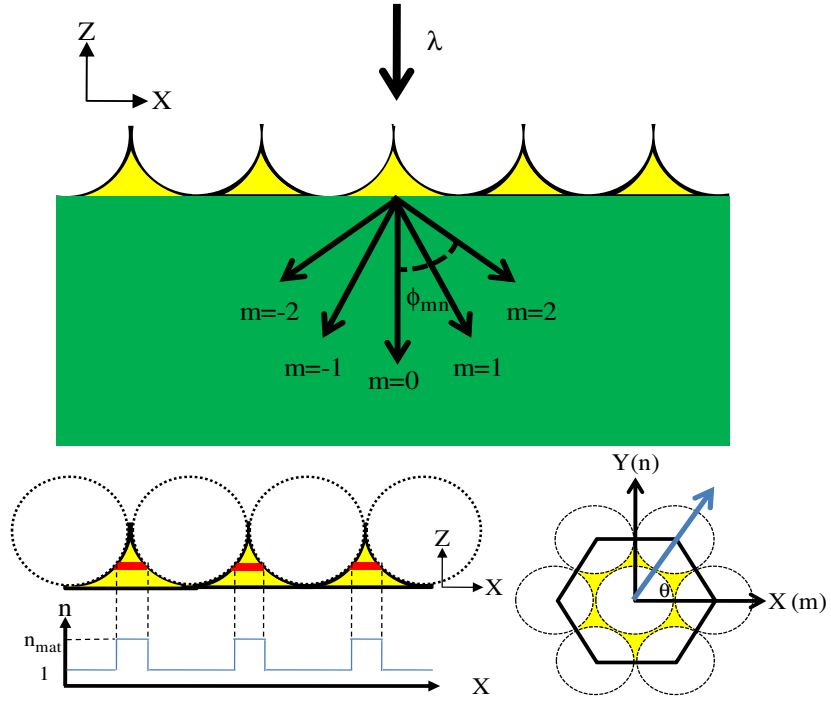

Figure 2. The schematic drawings of a hexagonal-nanoisland surface grating with an infinitely thick silicon (Si) layer.

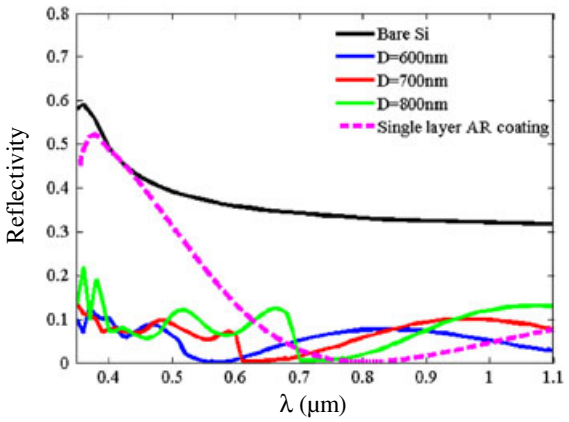

Figure 3. The calculated reflectivity spectra for $D = 600$, 700, 800 nm with a TiO_2 height $H = 300$ nm, a bare infinitely thick Si layer and Si with a 78-nm-thick silicon nitride (Si_3N_4) antireflection (AR) coating.

length for high-order diffraction is increased by a factor of $1/\cos\phi_{mn}$. To sufficiently increase optical absorption in Si, distributing the incident light intensity to high-order modes in the long-wavelength region is desired, as the absorption coefficient of Si is relatively small. The forward diffraction efficiency for each diffraction order (m, n), denoted as DE_{mn}, can be calculated using the RCWA method. Moreover, we define a new parameter, $\langle DE\rangle$ as a ratio of the diffracted power to the specular power, and express it as follows:

$$\langle DE\rangle = \frac{\sum_m \sum_n DE_{mn}}{DE_{00}}, \qquad (2)$$

where $\langle DE\rangle$ represents the summation of DE_{mn} for all diffraction orders other than DE_{00}. In this study, the summation is performed in the range from –4 to +4, where the diffraction efficiencies remain significant. As shown in Figure 5, $\langle DE\rangle$ is plotted as a function of wavelength for various sphere diameters D and a fixed aspect ratio $X = 0.4$. The absorption coefficient of Si is also plotted for reference. As D increases, the diffraction efficiency of high-order modes becomes significant at long wavelengths, where the absorption coefficient is small for Si. The summation of high-order diffracted power can be a few hundred times larger than zeroth order at specific wavelengths. Moreover, the peak of $\langle DE\rangle$ is also red-shifted as D increases. It is

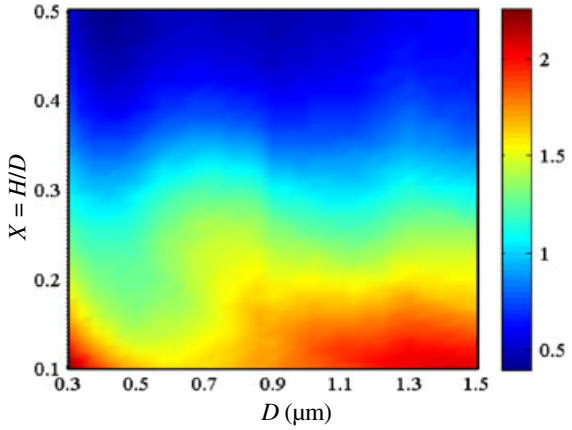

Figure 4. The calculated average reflectivity <*R*> as a function of the nanosphere diameter, *D* and the aspect ratio of TiO_2 nanoislands, *X*.

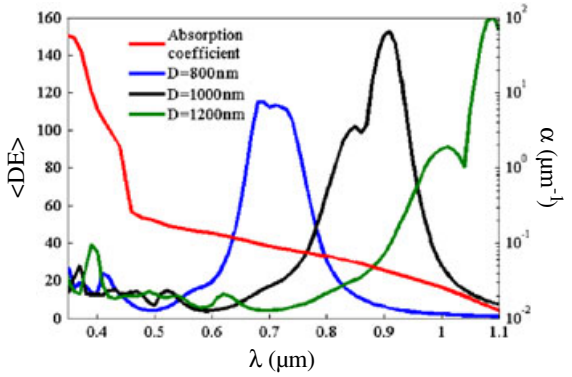

Figure 5. The diffraction power ratio of high-order modes to the zeroth order mode <*DE*>, and the absorption coefficient α of Si as a function of wavelength. The high orders become dominant in long wavelength as *D* increases.

worth noting that the first orders (0, 1) and (1, 0) are inhibited for the wavelength range of interest in the structure.

For a Si layer with a finite thickness, light trapping is more complicated than infinitely thick Si. In thin-film solar cells, the diffracted power can propagate within the absorbing layer if the diffracted wave satisfies the waveguide modes. The absorption is therefore enhanced when the strong coupling between the diffracted wave and the waveguide modes takes place. In the following section, the absorption efficiency of a finite Si layer is investigated. The enhanced absorption efficiency is contributed by both the antireflection effect and the coupling mechanism because of diffraction.

5. CELL ABSORPTION

In the previous sections, the surface reflection and the diffraction of the hexagonal PTP nanoislands were discussed for an infinitely thick Si layer. In this section, we consider the surface structure fabricated on a 2-μm-thick c-Si layer with an Al back-reflector, as previously illustrated in Figure 1. The short-circuit current density, J_{sc}, is characterized by the following equation under an assumption of 100% carrier collection:

$$J_{sc} = e\int_{350nm}^{\lambda g} A(\lambda) I_{AM1.5G}(\lambda) d\lambda, \quad (3)$$

where e is the electric charge, and A is the absorption spectrum of the 2-μm-thick c-Si layer. By monitoring the power stored in the active layer, the generated short-circuit current density can be obtained from Equation 3. For a 2-μm-thick bare silicon cell with an Al back-reflector, the calculated short-current density is 14.04 mA/cm^2. The optimized J_{sc} for a 2-μm-thick Si with a 70-nm-thick silicon-nitride AR coating is calculated to be 18.73 mA/cm^2. We also calculate a 2-μm-thick silicon cell with a double-layer AR coating composed of silicon dioxide and silicon nitride layers. The optimized J_{sc} for the double-layer AR coating is 18.97 mA/cm^2, where a 38-nm-thick silicon-dioxide layer is placed on top of a 50-nm-thick silicon-nitride layer. The double-layer AR

coating only slightly enhances the photocurrent compared with the single-layer, which exemplifies that the major efficiency limiting factor in a thin c-Si cell lies in the insufficient absorption length, instead of the deficiency of photon entry. To generate the most short-circuit current density for the proposed structure, we have calculated J_{sc} with respect to the aspect ratio X and the sphere diameter D of nanoislands. As shown in Figure 6, the optimal J_{sc}, 25 mA/cm^2 with $D = 740$ nm, $X = 0.5$, corresponding to an enhancement factor of 76.9% is obtained, compared with that of bare Si. Table I summarizes the optimized short-circuit current densities for 2-μm-thick bare silicon, that with a single-layer silicon-nitride AR coating, with a double-layer AR coating, and with the hexagonal PTP nanoislands. The respective enhancement of J_{sc} compared with the bare silicon is also presented. Compared with the calculated $J_{sc} = 20.6$ mA/cm^2 for a 2-μm-thick cell with a textured photonic crystal back-reflector and a DBR structure in Zeng *et al.* [4], the surface PTP nanoislands promise to boost the cell efficiency even further.

Combining the effects of antireflection and diffraction performed by the hexagonal PTP nanoislands, the absorption of Si is enhanced considerably over the entire absorption spectrum. The spectral short-circuit current density, $j_{sc}(\lambda)$ for optimized X and D is shown in Figure 7.

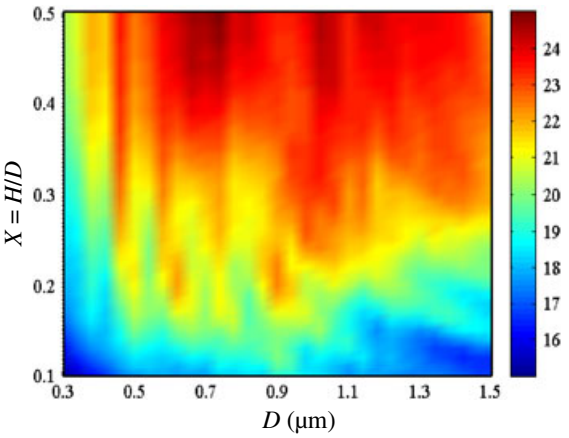

Figure 6. The calculated short-circuit current density J_{sc} (mA/cm^2) for a 2-μm-thick thin film crystalline Si as a function of structural parameters, X and D. J_{sc} is enhanced by the surface structure compared with $J_{sc} = 12.46$ mA/cm^2 for bare Si.

In silicon, the absorption length requires several hundred micrometers to completely absorb the photons near the Si band edge. For a 2-μm-thick silicon, which has a round-trip path length of 4 μm, only the wavelengths before the cutoff wavelength, $\lambda_c = 620$ nm can be completely absorbed. Before the cutoff wavelength, the enhancement is contributed by the antireflection effect of nanoislands. After the cutoff wavelength, the enhancement arises from both the antireflection and diffraction effects. Within the range of $\lambda = 620$–700 nm, the high-order diffraction ratio, <*DE*>, substantially results in a peak current density in the entire spectrum. In summary, a 28.2% of the enhanced photocurrent density is benefited before the cutoff wavelength, whereas 71.8% is contributed after the cutoff.

We further investigate the angular short-circuit current density of the PTP nanoislands with the optimized parameters ($D = 740$ nm, $X = 0.5$) at different angles of incidence (AOIs). The antireflection and diffraction properties of the PTP nanoislands strongly depend on the AOI. The diffraction efficiencies and angles for high-order modes vary with the AOI and consequently change the absorption efficiency of the silicon layer. The angular short-circuit current density, $J_{sc}(\vartheta)$ is characterized by the following equation:

$$J_{sc}(\vartheta) = e\int_{350nm}^{\lambda g} A(\vartheta) I'_{AM1.5G} d\lambda \quad (4)$$

Where ϑ is the AOI with respect to the surface normal, $I'_{AM1.5\ G}$ is the normal component of the incident photon flux density under an AM1.5 G illumination condition, that is, $I'_{AM1.5G} = I_{AM1.5\ G}\cos(\vartheta)$. Figure 8 shows the calculated angular short-circuit current density of cells with PTP nanoislands, a single-layer AR coating, and a double-layer AR coating. The calculation results depict an outstanding photocurrent improvement at large AOIs for PTP nanoislands. The largest $J_{sc} = 26.49$ mA/cm^2 is found at the AOI of 6°, which is attributed to a sufficient coupling of high-order diffraction modes to the guided mode of silicon. The ripples in the curve hence arise from strong couplings between the two types of modes at specific AOIs.

6. CONCLUSION

A novel front-surface nanoisland structure, which combines the functions of antireflection and light trapping was

Table I. Comparisons of the short-circuit current density (J_{sc}) and the J_{sc} enhancement for 2-μm-thick crystalline silicon cells with various absorption enhancement techniques.

Structure	J_{sc} in mA/cm^2 (350–1100 nm)	J_{sc} enhancement (350–1100 nm)
Silicon without any AR treatment	14.04	–
Silicon with a single-layer (Si_3N_4) AR coating	18.73	33.4%
Silicon with a double-layer (SiO_2/Si_3N_4) AR coating	18.97	35.1%
Silicon with optimized PTP nanoislands	25.00	76.9%

AR, antireflection; PTP, parabolic-triangular-pyramidal

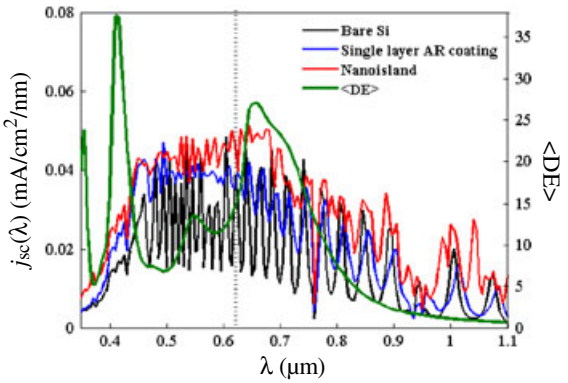

Figure 7. The calculated short-circuit current density spectra for 2-μm-thick silicon solar cells with various AR treatments. The vertical line indicates the cutoff wavelength for round-trip absorption length (4 μm). The current density is essentially contributed by high-order diffractions for $\lambda = 620$–700 nm.

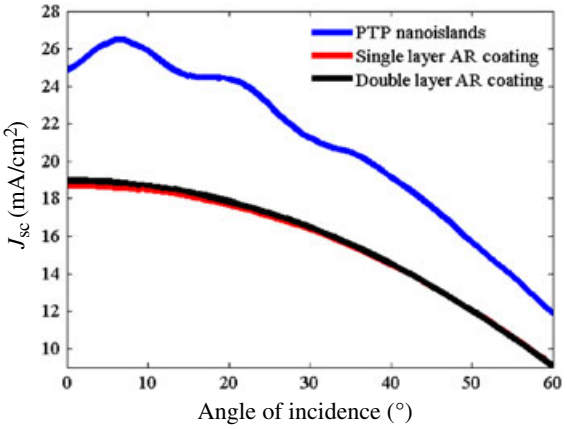

Figure 8. The calculated angular short-circuit current densities for 2-μm-thick Si solar cells with parabolic-triangular-pyramidal nanoislands ($D = 740$ nm, $X = 0.5$), a single-layer AR coating, and a double-layer AR coating.

systematically investigated. The nanostructure was fabricated using polystyrene colloidal lithography, which is a scalable and cost-effective process for large-area production. The nanoislands exhibited the properties of antireflection and light trapping because of gradient effective refractive indices and the periodicity, respectively.

In an infinitely thick silicon layer where light trapping is not required, the PTP nanoislands suppress the optical reflection by 60.5% with a sphere diameter $D = 420$ nm, an aspect ratio $X = 0.5$, compared with a single layer AR coating. For thin-film silicon where light trapping is needed, the surface hexagonal nanoisland grating sufficiently diffracts the incident light to high-order modes, which increases the optical path length for long-wavelength photons. Combining the antireflection and diffraction effects provided by the surface structure, we calculated the short-circuit current density at normal incidence and oblique incident angles for a 2-μm-thick crystalline Si solar cell. The solar cell with optimized structural parameters, D = 740 nm and a height of TiO_2 islands H = 370 μm, provides the largest $J_{sc} = 25$ mA/cm^2, corresponding to a 76.9% enhancement compared with that of a bare c-Si solar cell. Moreover, the structure shows significant photocurrent improvement at large angles of incidence than the single-layer and double-layer AR coatings, which promises sufficient sunlight harvesting for the entire day.

REFERENCES

1. Tao M, Zhou WD, Yang HJ, Chen L. Surface texturing by solution deposition for omnidirectional antireflection. *Applied Physics Letters* 2007; **91**: 081118. doi: 10.1063/1.2775805.
2. Bermel P, Luo C, Zeng L, Kimerling LC, Joannopoulos JD. Improving thin-film crystalline silicon solar cell efficiencies with photonic crystals. *Optics Express* 2007; **15**: 16986–17000.
3. Zeng L, Bermel P, Yi Y, Alamariu BA, Broderick KA, Liu J, Hong C, Duan X, Joannopoulos J, Kimerling LC. Demostration of enhanced absorption in thin film Si solar cells with textured photonic crystal back reflector.

Applied Physics Letters 2008; **93**: 221105. doi: 10.1063/1.3039787.

4. Feng NN, Michel J, Zeng L, Liu J, Hong CY, Kimerling LC, Duan X. Design of highly efficient light trapping structures for thin-film crystalline silicon solar cells. *IEEE Transactions on Electron Devices* 2007; **54**(8): 1926 – 1933.
5. Zhou D, Biswas R. Photonic crystal enhanced light-trapping in thin-film solar cells. *Journal of Applied Physics* 2008; **103**: 093102. doi: 10.1063/1.2908212.
6. Green MA, Basore PA, Chang N, Clugston D, Egan R, Evans R, Hogg D, Jarnason S, Keevers M, Lasswell P, O'Sullivan J, Schubert U, Turner A, Wenham SR, Young T. Crystalline silicon on glass (CSG) thin-film solar cell modules. *Solar Energy* 2004; **77**: 857– 863.
7. Sun C-H, Brian JH, Bin J, Peng J. Biomimetic subwavelength antireflective gratings on GaAs. *Optics Letters* 2008; **33**(19): 2224 – 2226.
8. Chen HL, Chuang SY, Lin CH, Lin YH. Using colloidal lithography to fabricate and optimize sub-wavelength pyramidal and honeycomb structures in solar cells. *Optics Express* 2007; **15**(22): 14793 – 14803.
9. Moharam MG, Gaylord TK. Rigorous coupled-wave analysis of metallic surface-relief gratings. *Journal of the Optical Society of America A* 1986; **3**(11): 1780 – 1787.
10. Yu P, Chang CH, Chiu CH, Yang CS, Yu JC, Kuo HC, Hsu SH, Chang YC. Efficiency enhancement of GaAs photovoltaics employing antireflective indium tin oxide nanocolumns. *Advanced Materials* 2009; **21**: 1618 – 1621.
11. Chiu CH, Yu P, Chang CH, Yang CS, Hsu MH, Kuo HC, Tsai MA. Oblique electron-beam evaporation of distinctive indium-tin-oxide nanorods for enhanced light extraction from InGaN/GaN light emitting diodes. *Optics Express* 2009; **17**(23): 21250 – 21256.
12. Bass M, DeCusatis C, Li G, Mahajan VN, Stryland EV. *Handbook of Optics*, 3rd edition, Vol. **4**. McGraw-Hill 2009.
13. Ho PKH, Thomas DS, Friend RH, Tessler N. All-polymer optoelectronic devices. *Science* 1999; **285**: 233 – 236.
14. Macleod HA. *Thin-Film Optical Filters*. Institute of Physics Publishing: Bristol, 2001; 641 pages.
15. Brendel R. *Thin-Film Crystalline Silicon Solar Cells*. Wiley-VCH: Weinheim, 2003; 287 pages.
16. ASTMG173-03, Standard Tables for Reference Solar Spectral Irradiances, ASTM International: West Conshohocken, Pennsylvania, 2005).
17. Ochiai T, Sakoda K. Dispersion relation and optical transmittance of a hexagonal photonic crystal slab. *Physical Review B* 2001; **63**: 125107.